0026-895X/09/7501-1–12$20.00
MOLECULAR PHARMACOLOGY
Vol. 75, No. 1
51938/3423246

Mol Pharmacol 75:1–12, 2009
Printed in U.S.A.

MINIREVIEW

Topology of Class A G Protein-Coupled Receptors: Insights Gained from Crystal Structures of Rhodopsins, Adrenergic and Adenosine Receptors

Debarshi Mustafi and Krzysztof Palczewski

Department of Pharmacology, Case Western Reserve University, Cleveland, Ohio

Received September 9, 2008; accepted October 21, 2008

ABSTRACT

Biological membranes are densely packed with membrane proteins that occupy approximately half of their volume. In almost all cases, membrane proteins in the native state lack the higher-order symmetry required for their direct study by diffraction methods. Despite many technical difficulties, numerous crystal structures of detergent solubilized membrane proteins have been determined that illustrate their internal organization. Among such proteins, class A G protein-coupled receptors have become amenable to crystallization and high resolution X-ray diffraction analyses. The derived structures of native and engineered receptors not only provide insights into their molecular arrangements but also furnish a framework for designing and testing potential models of transformation from inactive to active receptor signaling states and for initiating rational drug design.

G protein-coupled receptors (GPCRs), composed of seven transmembrane helices, are the largest superfamily of proteins in the human body. Disruption of most individual GPCR genes in mouse models is not lethal or developmentally harmful because genes encoding receptors responding to the same ligand(s) are highly redundant and/or encode regulatory proteins for physiological processes that can be controlled by different cellular mechanisms in case of failure. GPCRs, however, modulate almost all physiological processes because they are ubiquitous and largely located in plasma membranes, where they are readily accessible to endogenous signaling molecules, making them extremely attractive drug targets. The human genome sequence (Lander et al., 2001; Venter et al., 2001) indicates that of the ~35,000 human genes, ~720 encode GPCRs, of which ~400 are expected to be potential drug targets (Kroeze et al., 2003). GPCR agonist and antagonist drugs have been successfully used to treat patients with a broad spectrum of diseases owing to the large diversity of involved receptors (Drews, 2000; Wise et al., 2002). For example, common human disorders associated with vision (involving rhodopsin mutations; Menon et al., 2001), the cardiovascular system (caused by β_1-adrenergic receptors; Drake et al., 2006), asthma (attributable to β_2-adrenergic receptors; Kawakami et al., 2004), and strokes and cerebral hypoperfusion (altered adenosine A_{2A} receptor function in accompanying heart disease) all involve aberrant GPCR signaling. Identifying the pathophysiological roles of these potential drug targets is fundamentally dependent on understanding their inherent structures and three-dimensional ligand-protein interactions (Klabunde and Hessler, 2002). Detailed structural interactions between ligands and GPCRs are largely unresolved because of the inherent difficulty of membrane protein crystallization (Loll, 2003) despite new high-throughput technologies designed to limit the amounts of sample required (Hansen et al., 2002, 2006; Li et al., 2006).

Elucidation of the first mammalian GPCR structure of

This research was supported by National Institutes of Health grants EY09339, GM079191, and by an unrestricted grant from Amgen Inc and Sandler Program for Asthma Research. D.M. was supported in part by the CWRU Medical Scientist Training Program (MSTP) and National Institutes of Health grant T32-GM007250.

Article, publication date, and citation information can be found at http://molpharm.aspetjournals.org.

doi:10.1124/mol.108.051938.

ABBREVIATIONS: GPCR, G protein-coupled receptor; MII, metarhodopsin II; MI, metarhodopsin I; CGS21680, 2-[*p*-(2-carboxyethyl)phenethylamino]-5′-*N*-ethylcarboxamidoadenosine; AR, adrenergic receptor; ZM241385, 4-{2-[7-amino-2-(2-furyl)[1,2,4]triazolo-[2,3-*a*][1,3,5]triazin-5-ylamino]ethyl}phenol.

native bovine rhodopsin (Palczewski et al., 2000) and subsequent higher resolution structures (Li et al., 2004; Okada et al., 2004; Stenkamp, 2008) have opened the way to probe ligand binding sites and assess structure-function relationships for these membrane proteins (Lu et al., 2002; Hubbell et al., 2003; Park et al., 2004). The newest X-ray defined coordinates encompass all amino acids and post-translational modifications (Table 1). A mutant recombinant bovine rhodopsin structure solved at lower resolution (3.4 Å) than native rhodopsin (2.2 Å) has also been reported (Standfuss et al., 2007) (Table 1), and it highlights the possibility of using recombinant proteins for structural studies, as developed recently for adrenergic and adenosine receptors. Moreover, the structure of isorhodopsin was solved in which the native 11-*cis*-retinal of rhodopsin is replaced with the analog, 9-*cis*-retinal (Nakamichi and Okada, 2007; Nakamichi et al., 2007). No significant structural differences were noted between rhodopsin and isorhodopsin. The X-ray-defined structure of bovine rhodopsin initiated homology modeling of GPCRs (Filipek et al., 2003b; Patny et al., 2006) to understand the structures of other functionally important GPCRs and use them for rational drug design (Becker et al., 2003). Despite these efforts, the above methods failed to predict models and possible ligands efficiently for therapeutic purposes (Deupi et al., 2007). The only structural features common to all GPCRs are their seven transmembrane-spanning α-helical segments connected by alternating intracellular (C-) and extracellular (E-) loops, with the amino terminus located on the extracellular side and the carboxyl terminus on the intracellular side. Significant sequence homology is found, however, within several subfamilies of GPCRs engaged in redundant or unique functions (Gether, 2000). These typically are classified by the presence of specific motifs, ligand sizes, relationships to a reference receptor, and other criteria. The three major GPCR subfamilies in vertebrates include those related to rhodopsin, adrenergic, and adenosine receptors, totaling ~280 GPCRs (Kroeze et al., 2003). These receptors can be classified as those that show a highly conserved sequence homology of an Asp-Arg-Tyr motif on the intracellular side of the C-III loop (class A), the secretin-receptor family (class B), and those related to metabotropic glutamate receptors (class C; Gether, 2000). X-ray crystallography of structural forms of native rhodopsins, mutant β_1-adrenergic, and engineered β_2-adrenergic and A_{2A} adenosine receptors have been solved at high resolution. This review focuses on the elucidation of six new class A GPCR structures and how their structural features differ slightly from those existing in native bovine rhodopsin. Different motifs specific to each new structure are featured that confer its unique ligand specificity and activity. Also addressed are structural artifacts attributable to the use of mutations and fusion proteins for X-ray crystallography and the future implications of structural work for cellular signaling mechanisms and drug design.

Different Photointermediates of Rhodopsin

Rhodopsin is a GPCR expressed in rod retinal photoreceptors that plays a key role in vision by converting light into a cascade of biochemical transformations called phototransduction (Filipek et al., 2003a; Palczewski, 2006). Rhodopsin was the first crystallized GPCR (Okada et al., 2000; Palczewski et al., 2000), and subsequent work resulted in crystallization of rhodopsin photointermediates that improved understanding of the chromophore transformation cycle. The membrane embedded chromophore contained in rhodopsin is 11-*cis*-retinal. This is covalently bound to the inactive opsin protein by a Lys residue (Lys296) in helix VII via a protonated Schiff base. Upon absorption of a photon, isomerization of this chromophore to an all-*trans* conformation induces changes in the opsin structure, ultimately converting it from an inactive to an activated signaling state. The last form of this receptor, known as metarhodopsin II (MII or R*), relays the activating changes to the retinal G protein, transducin (G_t), that in turn initiates the series of biochemical reactions culminating in a neuronal signal.

As the chromophore converts to the all-*trans* conformation during photoactivation, rhodopsin progresses through a series of photointermediates. The first structurally characterized photointermediate, bathorhodopsin, thermally relaxes to the blue-shifted intermediate bathorhodopsin, followed by lumirhodopsin and then metarhodopsin I (MI). In MI, the all-*trans*-retinal chromophore remains bound to opsin. However, during the MI-to-MII transition, the all-*trans*-retinylidene Schiff base becomes deprotonated. MII, the signaling state capable of G protein activation, ultimately decays to form free all-*trans*-retinal and opsin. It is noteworthy that two forms of MI and MII have been found, MIa/MIb and MIIa/MIIb, both in a pH-dependent equilibrium; MIIb is the only MII partner capable of activating G_t (Okada et al., 2001; Schertler, 2005; Ridge and Palczewski, 2007).

Because photoactivation of rhodopsin involves formation of a series of reaction intermediates having different shapes and dissimilar retinal ligands, different forms of rhodopsin crystals should be ideal for studying the mechanism of GPCR activation. With a high light-absorption coefficient, the intrinsic chromophore of rhodopsin is a sensitive indicator of conformational changes because of its sensitivity to minor changes in the first, second, and even the third environmental shell surrounding the chromophore binding pocket. This property is harnessed by nature, which uses binding of an identical chromophore to different opsins to regulate the λ maximum absorption, or the so-called opsin shift, to provide a molecular mechanism for color vision. Because protonated retinylidene interacts with its counter-ion, minimal changes in the distance between this pair can produce large changes in the λ maximum, irrespective of changes in the overall protein structure (Fig. 1). This hypothesis is well supported by rhodopsin mutants with engineered disulfide bridges connecting helices to prevent large conformational changes that both spectrally and in G protein assays achieve an MII state (Yu et al., 1995). Thus, identification of rhodopsin intermediates by their spectral properties alone constitutes a fundamental problem if changes in the λ maxima of these photointermediates are considered indicative of alterations in protein conformation rather than just a reflection of chromophore status. Three-dimensional structures of bathorhodopsin and lumirhodopsin were obtained after trapping these photolyzed states at low temperatures, whereas that of MI was resolved by using electron crystallography of two dimensional crystals (Ruprecht et al., 2004; Nakamichi and Okada, 2006a; Nakamichi and Okada, 2006b). A structure of the deprotonated photoactivated state of rhodopsin, resembling MII, has also been elucidated (Salom et al., 2006b).

TABLE 1
Characteristics of class A G protein-coupled receptor crystal structures

Structure	Release Year	PDB ID	Resolution/ Space Group	Mutations	Truncations	Unresolved Residues	Ligands/complexes or fusions/ other alternations
Bovine rhodopsin	2000	1f88	2.80 Å/$P4_1$			Gln236-Glu239, Leu328-Ala333	11-*cis*-Retinal
Bovine rhodopsin[a]	2003	1gzm	2.65 Å/$P3_1$			Pro327-Gly329, Ala333-Ala348	11-*cis*-Retinal
Bovine rhodopsin	2004	1u19	2.20 Å/$P4_1$				11-*cis*-Retinal
9-*cis*-Bovine rhodopsin (isorhodopsin)	2007	2ped	2.95 Å/$P4_1$				9-*cis*-Retinal
Recombinant bovine rhodopsin mutant	2007	2j4y	3.40 Å/$P3_1$	N2C, D282C		Leu328-Ala348	11-*cis*-Retinal
Squid rhodopsin	2008	2z73	2.50 Å/$P6_2$		Ser359-Ala448	Met1-Asn8	11-*cis*-Retinal
Squid rhodopsin	2008	2ziy	3.70 Å/C 2 2 2_1	V18I	Met374-Ala448	Gly2-Arg3	11-*cis*-Retinal
Bovine bathorhodopsin	2006	2g87	2.60 Å/$P4_1$				all-*trans*-Retinal
Bovine lumirhodopsin	2006	2hpy	2.80 Å/$P4_1$				all-*trans*-Retinal
Bovine meta II-like rhodopsin (photoactivated)	2006	2i37	4.15 Å/$P3_112$			Val230-Gln238, Lys311-Phe313, Asp330-Ala348	all-*trans*-Retinal
Opsin	2008	3cap	2.90 Å/H3			Pro327-Ala348	
Opsin	2008	3dqb	3.20 Å/H 3 2	K341L		Pro327-Ala348	C-terminal peptide (11 mer) derived from the Gα subunit of transducin
Turkey β_1-Adrenergic receptor	2008	2vt4	2.70 Å/P1	R68S, M90V, C116L, Y227A, A282L, F327A, F338M, C358A, and deglycosylated	Asp2-Ser32, Cys244-Arg271, Ala368-Ala496	Met1-Gly2, Ala33-Gln39, Arg239-Arg243, Ala272-Met283, Pro360-Leu367	Cyanopindolol
Human β_2-adrenergic receptor	2007	2r4r	3.40 Å/C 2 (C 121)		Tyr366-Leu413	Met1-Met336, Lys60, Ala91-Glu107, Ser165-Ala202, Gln243-Lys263, Val292-Leu310, Ala349-Gly365	Carazolol; Fab attachment to C-III loop and portion of helix VII
Human β_2-adrenergic receptor	2007	2rh1	2.40 Å/C 2 (C 121)	N187E (elimination of glycosylation site), Gln231-Ser262 (replaced by amino acids 2–161of T4 lysozyme), C1054T and C1097A (lysozyme)	Tyr366-Leu413	Met1-Arg28, Arg343-Gly365	Carazolol; T4 lysozyme chimera to C-III loop
Human β_2-adrenergic receptor	2008	3d4s	2.80 Å/$P2_12_12_1$	E122W, N187E (elimination of glycosylation site), Gln231-Ser262 (replaced by amino acids 2–161of T4 lysozyme), C1054T and C1097A (lysozyme)	Arg349-Leu413	Met1-Val31, Arg343-Lys348	Timolol; T4 lysozyme chimera to C-III loop
Human A_{2A} adenosine receptor	2008	3eml	2.60 Å/P1 2_1 1	Leu209-Ala221 (replaced by amino 2–161 acids of T4 lysozyme), C1054T and C1097A (lysozyme)	Ala317-Ser412	Met1-Pro2, Gln148-Ser156, Gln311-Ala316	ZM241385 antagonist; T4 lysozyme chimera to C-III loop

[a] Corrected space group by Stenkamp (2008).

The first intermediate trapped after light absorption by rhodopsin is bathorhodopsin; this occurs within a few hundred femtoseconds at room temperature. X-ray diffraction was used to calculate the difference in densities corresponding to the retinal. The overall residual structural changes are slight, but retinal does undergo a small displacement in the β-ionone ring defined by the binding pocket that has room on the extracellular side of the ring (Fig. 1). Studies suggest that the 11-*cis*-retinal binding pocket is designed to achieve a dual function (i.e., retain retinal as an inverse agonist in the dark and allow its efficient photoconversion to an agonist upon exposure to light) (Nakamichi and Okada, 2006a).

Bathorhodopsin crystals were illuminated with visible light and warmed, resulting in a gradual conversion to lumirhodopsin, the second trappable intermediate. Retinal in lumirhodopsin assumes an all-*trans* structural conformation. Compared with retinal in bathorhodopsin, there is relaxation of the curved polyene chain. This process is proposed to be the key step in transferring stored photon energy to the surrounding protein moiety by converting the 11-*cis*-retinylidene inverse-agonist to an all-*trans* agonist (Nakamichi and Okada, 2006b) (Fig. 1).

An equilibrium is formed between the later photointermediates, MI and MII. MII corresponds to the fully activated receptor, which binds to and activates the heterotrimeric G_t. MI was studied by freeze-trapping and electron microscopy. Density maps revealed that MI formation does not involve large movements or rotations of rhodopsin's helices but rather, as noted with the other photointermediates, conformational changes localized around the chromophore binding pocket. At this stage, photon energy is fully transferred to the protein-chromophore complex and the excess of energy dissipated as oscillation vibrations (Ruprecht et al., 2004).

The subsequent transformation from MI to MII is driven by enthalpy. The inherent instability of rhodopsin in its photoactivated deprotonated state required development of a purification protocol and crystallization conditions that was capable of withstanding photoactivation (Salom et al., 2006a). This advance permitted the growth of ground state crystals, albeit at lower resolution (4.1 Å) than other rhodopsin structures, that upon exposure to light transformed rhodopsin into a photoactivated deprotonated intermediate resembling the MII biological state. Unlike the other rhodopsin structures, the photoactivated structure did not have residues Val230 to Gln238, Lys311 to Phe313, and Asp330 to Ala348 resolved (Table 1) as a result of low resolution and/or flexibility of structural regions. Nonetheless, fine changes were noted in this photoactivated structure (Fig. 2, A and B). The X-ray crystallographic data elucidated that photoactivation primarily causes relaxation of the C-III loops, before the chromophore is hydrolyzed from the binding site and rhodopsin is regenerated from opsin by freshly synthesized 11-*cis*-retinal (Travis et al., 2007). A higher resolution structure of this intermediate is needed.

Crystallographic snapshots of these photointermediates help elucidate the process of chromophore turnover and indicate that the entire activation process entails subtle changes in the overall structure of rhodopsin. The importance of minimal changes found in the photoactivated structures is further highlighted by the potential for dimers of rhodopsin to explain its physiological function. Nonphysiological dimers of rhodopsin can be found in its first three-dimensional (3D) crystals, where the two subunits are related by a rotation of 180° about an axis in the plane of the membrane that seem to be induced by experimental crystallization conditions (Palczewski et al., 2000; Okada et al., 2001; Teller et al., 2001). However, the new crystal form of the photoactivated structure unveiled a possible physiologically relevant dimer rhodopsin interface. The photoactivated crystal reveals that the dimer is stabilized by a series of intermolecular contacts previously observed in other 3D crystals but rotated by 180° around a hydrophobic center (Salom et al., 2006b). These results are consistent with data obtained by atomic force microscopy and molecular modeling (Fotiadis et al., 2003; Liang et al., 2003; Filipek et al., 2004; Liang et al., 2004). Moreover, the finding of dimeric rhodopsin crystals offers a potential explanation for its higher-order organization in native membranes and provides a template to study GPCR activation by crystallography (Müller et al., 2008). Structural similarity between the activated and ground states shows that rhodopsin is a good template for homology models of other GPCRs.

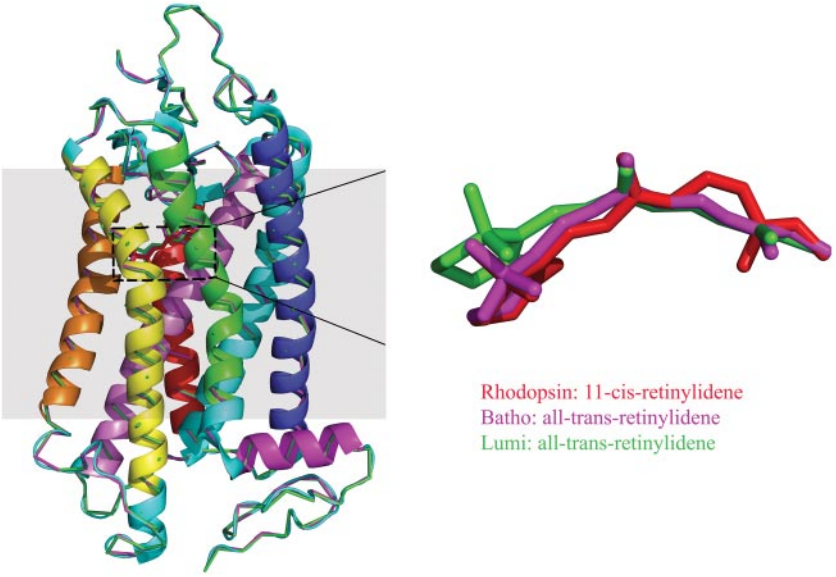

Fig. 1. Structural transformations of rhodopsin during photolysis. Alignment of the first three photointermediates, bovine rhodopsin colored by helix: helix I (blue), helix II (cyan), helix III (violet), helix IV (red), helix V (orange), helix VI (yellow), helix VII (green), and helix 8 (magenta); bovine bathorhodopsin (magenta); and bovine lumirhodopsin (green) reveals that the most pronounced structural changes occur in the chromophore region (dashed rectangle). The chromophore from each of the three structures is shown on the right to highlight the changes as photolysis proceeds. Retinal is colored red for ground state rhodopsin, magenta for bathorhodopsin, and green for lumirhodopsin. From the ground state to bathorhodopsin, the $C_{11} = C_{12}$ bond adopts a *trans* configuration after illumination. From bathorhodopsin to lumirhodopsin, a conformational change in the β-ionone ring of the retinal is apparent. Changes in MII and opsin are more pronounced, with opsin showing slight side chain shifts of helices surrounding the chromophore binding site that allow retinal entry and exit as illustrated in Fig. 4.

We think that an urgent priority now includes the elucidation of the structural complexes of photoactivated rhodopsin with its partner proteins, G_t, rhodopsin kinase (GRK1), and arrestin. These structures will provide a truer physiologic perspective of how GPCRs achieve their signaling conformation(s). The complexity of these proteins, especially the G proteins, as well as the instability and heterogeneity of such complexes, will make these investigations extremely challenging. Unfortunately, "domain" approaches are not suitable for GPCR studies because their entire structures form one signaling domain. As illustrated by work with peptides encompassing different regions of GPCRs and interacting proteins, fragments of these receptors' partner proteins inadequately mimic the native proteins' interactions and their thermodynamic properties.

Comparison of Invertebrate and Vertebrate Structures: Squid versus Bovine Rhodopsin

In contrast to vertebrate vision, wherein signal transduction is mediated by the second messenger cyclic GMP, invertebrate phototransduction employs an inositol-1,4,5-triphosphate signaling cascade in which a G_q protein is stimulated by photoactivated rhodopsin (Terakita et al., 1998). Understanding the invertebrate visual transduction process was enhanced by discovery of the X-ray-defined structure of squid rhodopsin (Murakami and Kouyama, 2008). The large C terminus of squid rhodopsin was proteolytically removed, and the M1-N8 residues were not resolved (Table 1). Invertebrate rhodopsin forms a stable pigment with either 11-*cis*- or all-*trans*-retinylidene, so resolution of these structures constitutes an initial step in learning about the critical determinants protecting the chromophore from hydrolysis. Comparison of squid and bovine rhodopsin in a tetragonal $P4_1$ crystal (Okada et al., 2004) revealed that the most notable difference is in the C-III loop, a difference attributable to the extra sequence of squid rhodopsin in this region (Fig. 2, C and D). The C-III loop of bovine rhodopsin takes on different conformations in different crystal forms (Li et al., 2004; Stenkamp, 2008). Extensions of helices V and VI into the cytoplasmic medium are probably important structural motifs for specifying the coupling mode with G_q. Thus, squid rhodopsin provides insights into the differences in rhodopsin signaling mechanisms between vertebrates and invertebrates.

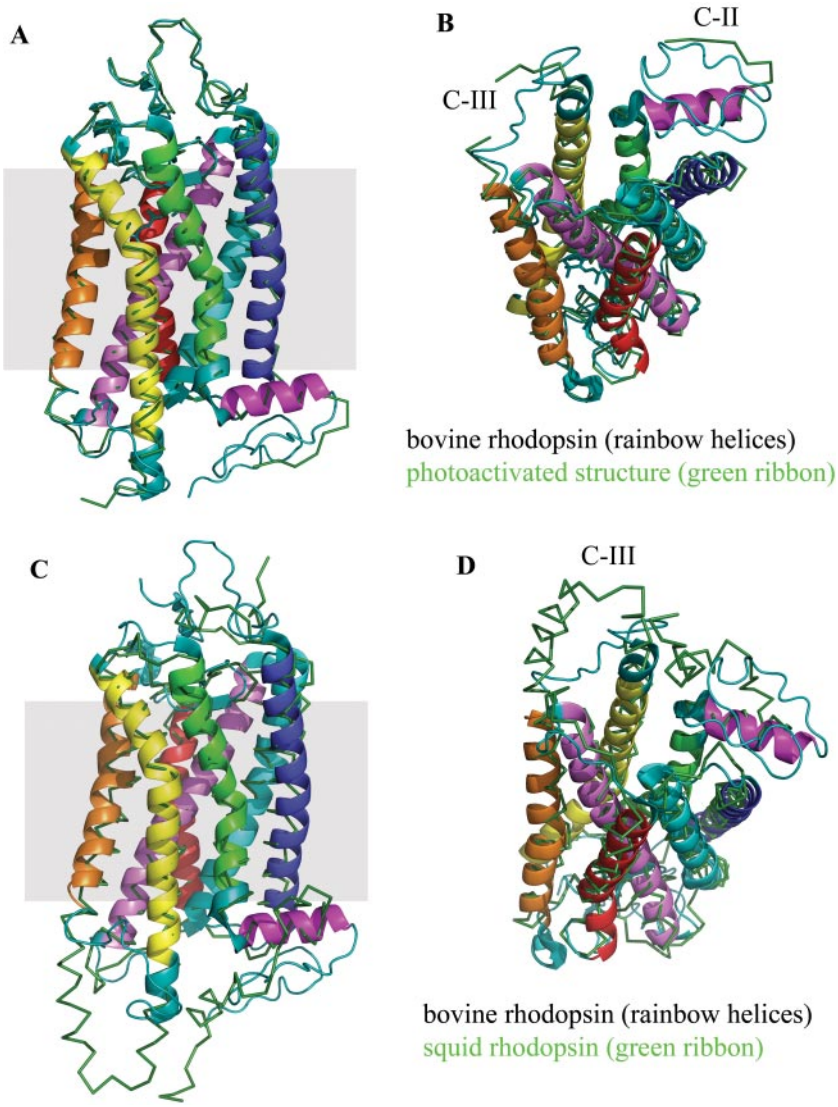

Fig. 2. Comparison of rhodopsin with the photoactivated state resembling the MII structure and squid rhodopsin. A, side view. Molecules are colored as the bovine photoactivated structure (green ribbon) and bovine rhodopsin by helix I (blue), helix II (cyan), helix III (violet), helix IV (red), helix V (orange), helix VI (yellow), helix VII (green), and helix 8 (magenta). These structures revealed smaller conformational changes than predicted from EPR studies. B, cytoplasmic view. Although the photoactivated structure resembling MII is structurally similar to that of the ground-state rhodopsin, portions of the C-II and C-III loops are disordered in the photoactive state. The C-III loop does not even follow the path of the loop found in the ground-state crystals. This difference may reflect the importance of these loops' dynamics in transducin activation. C, side view of squid rhodopsin is shown as a green ribbon overlying bovine rhodopsin colored by helix. D, these two structures show immense structural homology, with the most noticeable difference being the larger C-III loop in squid rhodopsin as a result of an extra sequence in that region. The difference in the C-III loop, involved in the binding of transducin, suggests that this may be an important structural motif for specifying different modes of coupling with G_q-type G proteins in invertebrate rhodopsins.

Understanding Chromophore Exchange in Vision: Opsin versus Rhodopsin

Native bovine opsin, an inactive form of rhodopsin lacking the chromophore, was crystallized (Park et al., 2008a; Scheerer et al., 2008) by optimizing the selective extraction of rhodopsin from rod cell disc membranes (Okada et al., 1998; Okada et al., 2000). This method enabled crystallization without any modification of the protein that might cause structural distortions. Structural examination of this opsin reveals only slight changes relative to rhodopsin for transmembrane helices I to IV. The most obvious differences are found in the region of transmembrane helices V to VII; these are especially prominent at the cytoplasmic ends of these helices and cause rearrangement of the C-II and C-III loops (Fig. 3, A and B). Furthermore, the ionic lock is broken in the opsin structure such that the rearranged cytoplasmic ends of transmembrane helices five and six are locked by two new interactions. Lack of the interacting prosthetic group of 11-*cis*-retinal causes a few distinct structural alterations in the retinal-binding pocket. Part of the space occupied by the β-ionone ring is filled in opsin by the side chain of Trp^{265}. In addition, lack of stabilizing residues to hold the polyene chain of the retinal in place causes helix III and the C-III loop to move slightly away from transmembrane helices V to VII. This allows the retinal-binding pocket to become wider toward the retinal attachment site of Lys^{296} (Park et al., 2008a; Scheerer et al., 2008). The C terminus of the opsin structure is not resolved from residues Pro327 to Ala348 (Table 1). However, a complex between opsin and the C-terminal peptide derived from α-subunit of G protein transducin optimized for tight binding was recently reported (Scheerer et al., 2008) (Table 1). In our opinion, further experiments are essential to show regeneration of opsin crystals back to rhodopsin with 11-*cis*-retinal chromophore because opsin is inherently unstable in detergents and unable to rebind chromophore (Buczyłko et al., 1996; McKibbin et al., 2007). This approach would also provide conclusive evidence that the crystal form reported is of true biologic relevance. The previously studied structure could represent opsin or a more stable conformation of opsin that can no longer be regenerated.

The two different openings of the retinal-binding site in opsin suggesting different retinal entrance and exit routes support the hypothesis that all-*trans*-retinal exits via a pathway differing from the entrance route and remains bound to an exit site (Schadel et al., 2003) with the opening between helices I and VII serving as a possible release structure for all-*trans*-retinal. The proposed uptake route between the extracellular ends of helices V and VI may be a general route of ligand uptake among GPCRs as evidenced by our current simulations and past chemical work. Amine ligands for the β_2-adrenergic receptor exhibit structural similarities to retinal and the aromatic carbazole ring of the inverse agonist, carazolol, could enter the ligand binding pocket at the opposite side of the E-III loop, between helice V and VI (Park et al., 2008a; Scheerer et al., 2008). Studies before the opsin structure was elucidated (Schadel et al., 2003) suggested the existence of a tunnel for retinal to traverse, but it was not until the opsin structure was solved that tunneling of the ligand could be confidently deduced. Use of the online software Caver (Petrek et al., 2006) allowed elucidation of the tunneling pathway for retinal into the binding pocket to covalently bind to Lys^{296} (Fig. 4). This shows two distinct sites, validating the hypothesis that the ligand enters and exits through different parts of the protein. The larger opening between helices V and VI (Fig. 4) is logical for the uptake of 11-*cis*-retinal, whereas an exit route for all-*trans*-retinal through the opening between helices I and VII also is realistic owing to its more sterically constricted tunneling configuration.

The β-Adrenergic and Adenosine Receptors

β_1-Adrenergic Receptor versus Rhodopsin. Rhodopsin and adrenergic receptors belong to class A, the largest and most studied of all GPCR classes. In a crystallized mutant form of the β_1-adrenergic receptor in complex with the high-affinity antagonist cyanopindolol, six residues were mutated (R68S, M90V, C116L, Y227A, A282L, F327A, F338M, and C358A), three regions were deleted (Asp2–Ser32, Cys244–Arg271, and Ala368–Ala496), and large portions of the structural Met1 to Gly2, Ala33 to Gln39, Arg239 to Arg243, Ala272 to Met283, and Pro360 to Leu367 regions

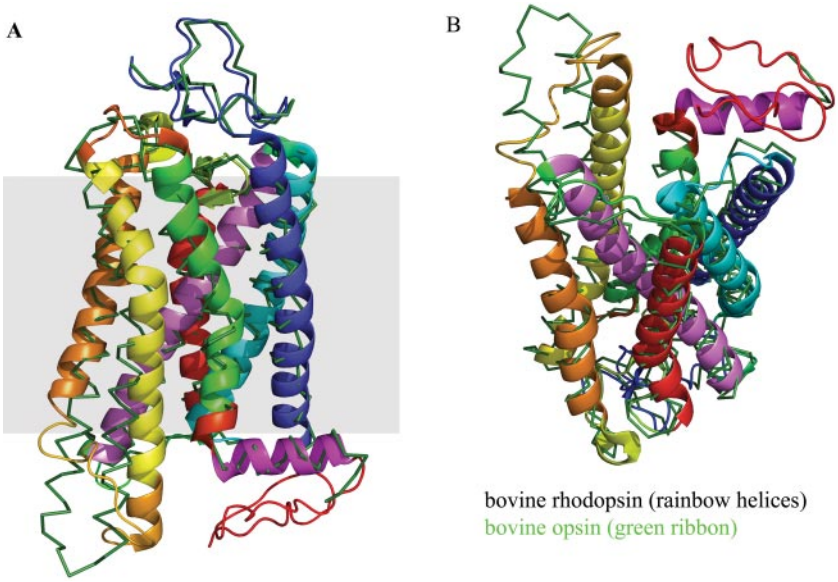

Fig. 3. Comparison of rhodopsin and opsin structures. A, side view. Molecules colored as bovine opsin II (green ribbon) and bovine rhodopsin by helix: helix I (blue), helix II (cyan), helix III (violet), helix IV (red), helix V (orange), helix VI (yellow), helix VII (green), and helix 8 (magenta). Despite overall helical plasticity, the structural overlay illustrates slight shifts in the side chains that could explain retinal entry/exit (see Fig. 4). B, cytoplasmic view. The opsin and rhodopsin structures show similar tracings of the cytoplasmic loops, but slight differences may indicate the importance of these loop movements in activation or relaxation back to the ground state.

were not resolved (Table 1). Despite the overall structural plasticity, the resulting modified structure has some parts that differ from those of native rhodopsins. In all GPCRs, C-II and C-III loops are believed to have a role in the binding, selectivity, and activation of G proteins, the C-II loop being important for the strength of the interaction and the C-III loop for specificity (Wong and Ross, 1994). The difference in the conformation of C-II loop also is important because this region is highly conserved between β_1- and β_2-adrenergic receptors, although it is poorly conserved between these structures and rhodopsin. In a mutated form of the turkey β_1-adrenergic receptor (Fig. 5), the C-II loop forms a short α-helix parallel to the membrane surface, whereas in both the mutant β_2-adrenergic receptor structures and in rhodopsin, this loop is in an extended conformation (Warne et al., 2008). The C-III loop is absent in the β_2-adrenergic receptor-T4 chimera crystal structure and sequestered by the Fab in the other β_2-adrenergic receptor structure. Destruction of important structural motifs like this probably has compromised the utility of these structures because they do not represent native conformations. Crystallographic artifacts may also change structural insights into ligand binding and thus adversely affect rational drug design. This alteration is reflected by the mutated turkey β_1-adrenergic receptor structure to which the natural agonists noradrenaline and isoprenaline bound more weakly by factors of 2470 and 650, respectively, than to the wild-type form (Warne et al., 2008).

β_2-Adrenergic Receptor versus Rhodopsin. The overall structure of the β_2-adrenergic receptor with its partial inverse agonist, carazolol, is similar to that of rhodopsin and the β_1-adrenergic receptor, with seven transmembrane helices and an eighth helix that runs parallel to the cytoplasmic face of the membrane (Fig. 6) (Cherezov et al., 2007; Hanson et al., 2008). However, the β_2-adrenergic receptor was highly engineered with E122W, N187E, Gln231 to Ser262 (replaced by amino acids 2 to 161 of T4 lysozyme) mutated in the protein, C1054T and C1097A mutated in the T4 lysozyme, and C-terminally Tyr366 to Leu413 truncated. Moreover, Met1 to Arg28 and Arg343 to Gly365 were not resolved in this structure (Table 1). Thus, we think that any detailed comparison with rhodopsin should be considered with caution. Even so, the structurally conserved helices provide a common core present throughout class A GPCRs, whereas the variable helices confer binding-site plasticity with a resulting architecture capable of binding a large spectrum of ligands. In particular, and in contrast to rhodopsin, the β_2-adrenergic receptor has a more open structure. Both forms of the fusion receptors show that the largest difference is in helix I, which is relatively straight and lacks the pro-induced kink found in rhodopsin; this feature may meet the need for an accessible ligand binding site in the β_2-adrenergic receptor. Differences in the arrangement of the C-loops of the transmembrane segments of the β_2-adrenergic receptor and rhodopsin may provide structural insights into basal receptor activity, given that rhodopsin has no detectable basal activity in contrast to the relatively high basal activity of the β_2-adrenergic receptor (Rasmussen et al., 2007). However, the β_2-adrenergic receptor-T4 chimera crystal displayed cholesterol-mediated dimeric contacts (Hanson et al., 2008) in a similar orientation as discussed for rhodopsin.

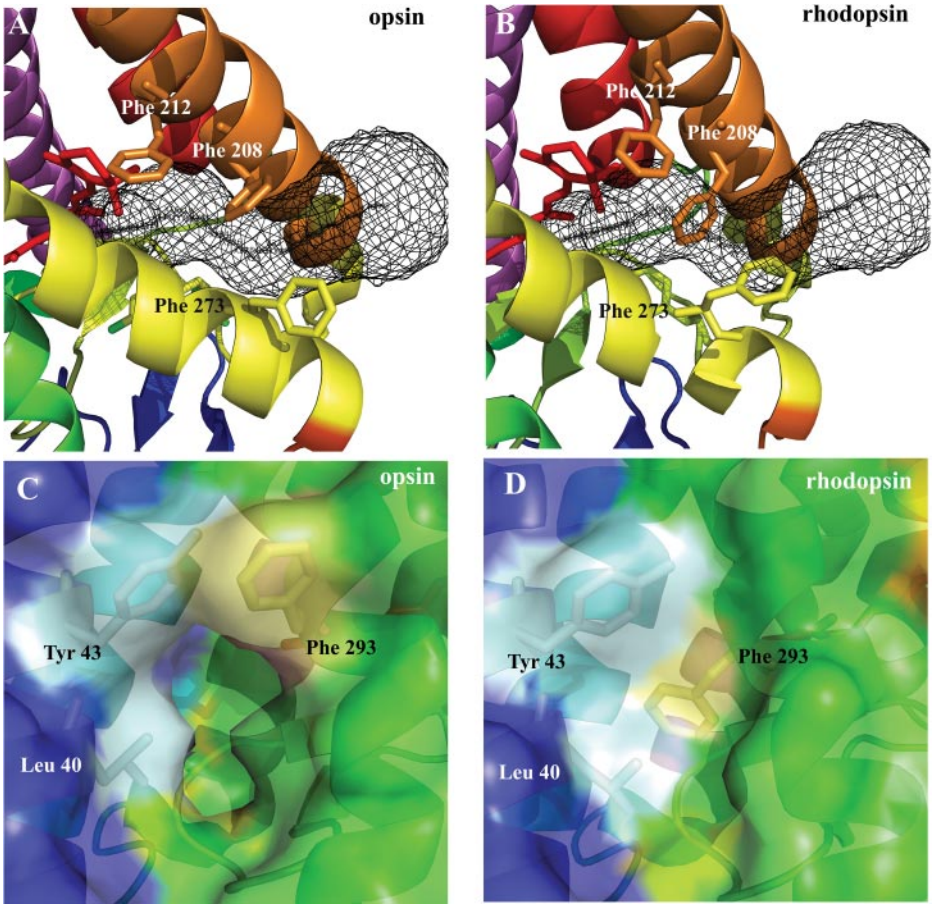

Fig. 4. Structural comparison between opsin and rhodopsin illustrating a pathway for retinal exchange. The opsin structure shows two different openings to the retinal-binding pocket (i.e., one between the extracellular ends of helice V and VI and the other between helices I and VII. These openings suggest different chromophore entrance and exit routes. Both bovine opsin and bovine rhodopsin are colored by helix: helix I (blue), helix II (cyan), helix III (violet), helix IV (red), helix V (orange), helix VI (yellow), helix VII (green), and helix 8 (magenta), whereas retinal is depicted as red sticks. A, use of the online software Caver shows a tunneling path of retinal through an entry site between helix V and helix VI of opsin, with three key Phe residues lining the path (Phe208, Phe212, and Phe273). B, this retinal entry path is blocked in rhodopsin as a result of shifts in helices V and VI that cause repositioning of these three key Phe residues. C, a distinct pathway for retinal exit from opsin is formed between helices I and VII and is illustrated as a clear hole in the solvent accessible surface. D, similar to the retinal entry pathway, the exit pathway is closed off in rhodopsin, most notably by a shift in Phe^{293}, as evidenced by the closed solvent accessible surface.

Information from the Fab/mutant β_2-adrenergic receptor complex also provides a global understanding of receptor topology, but the structure is less informative with regard to the precise receptor topology related to physiologic ligand interactions because its crystallization involved similar truncations (Tyr366–Leu413) and unresolved residues Met1 to Met36, Lys60, Ala91 to Glu107, Ser165 to Ala202, Gln243 to Lys263, Val292 to Leu310, and Ala349 to Gly365 (Table 1) as well as adaptation of the C-III loop to bind the Fab antibody fragment.

Adenosine Receptor versus Rhodopsin. Like the β_2-adrenergic receptor, the human A_{2A} adenosine receptor was crystallized after applying a T4L fusion strategy wherein most of the third cytoplasmic loop is replaced with lysozyme and the carboxyl-terminal tail (Ala317–Ser412) is truncated; the resulting structure also revealed that Met1 to Pro2, Gln148 to Ser156, and Gln311 to Ala316 were unresolved (Table 1). Despite these similarities, the adenosine receptor has a phospholipid bound in the cholesterol consensus motif. There is also evidence that may suggest that the fusion protein may have shifted its structure toward the activated state, as evidenced by an increased affinity for the subtype-selective agonist CGS21680 compared with the wild-type construct. The helical arrangement is similar among the human β_2AR, turkey β_1AR, and squid/bovine rhodopsin structures determined to date. However, the binding pocket of the A_{2A} adenosine receptor is shifted closer to helices VI and VII, compared with the position of the retinal and carazolol binding pocket in the vicinity of helices III, V, and VI. In addition, the E-II loop of the adenosine receptor differs considerably from its counterparts in β_2AR, β_1AR, and rhodopsin, in that it lacks any prominent secondary structural element and possesses three disulfide linkages with the E-I loop. This contributes to an extensive disulfide bond network

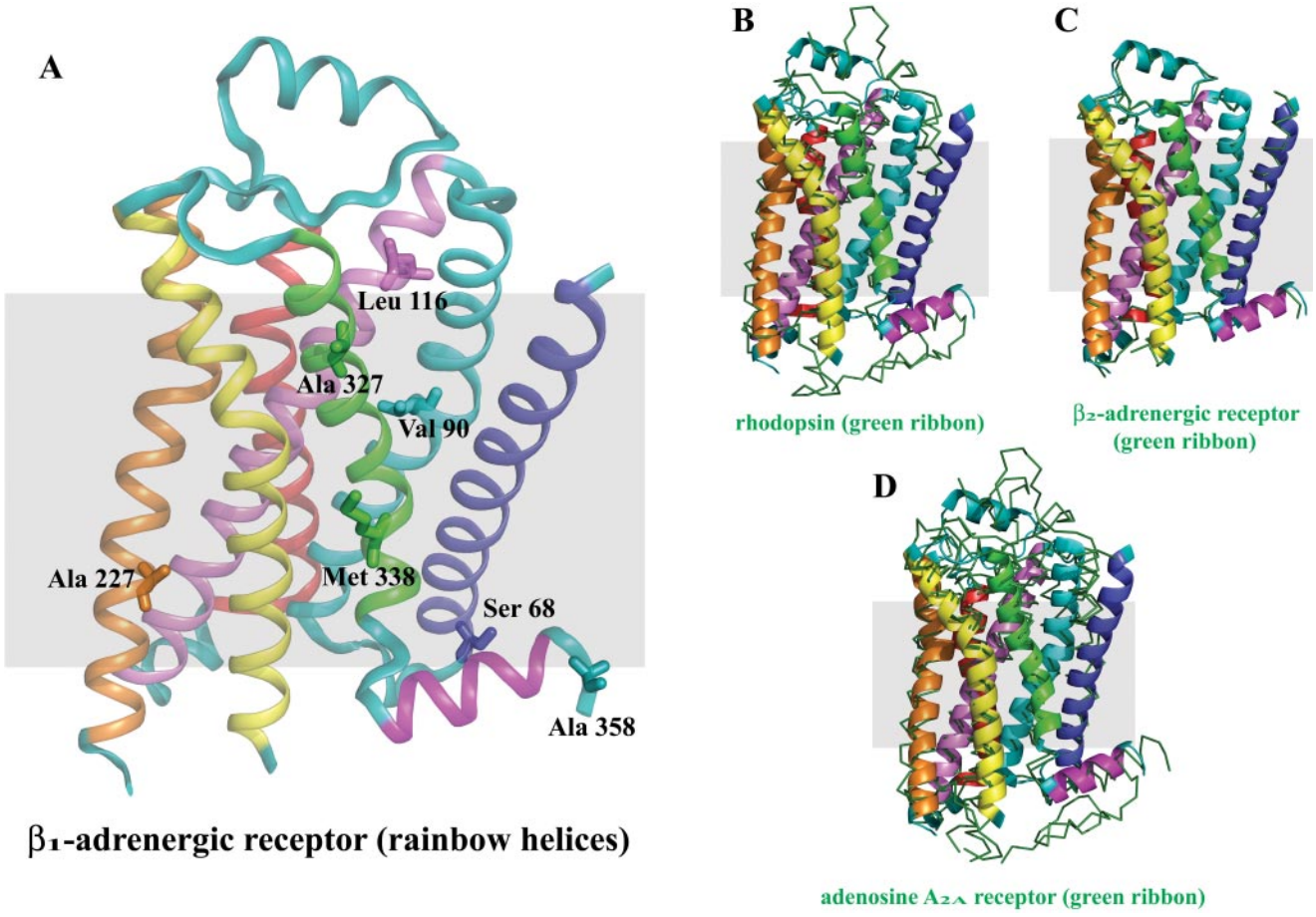

Fig. 5. Comparison of β_1-adrenergic receptor with rhodopsin, β_2-adrenergic receptor, and A_{2A} adenosine receptor structures. The turkey β_1-adrenergic receptor was mutated to facilitate its crystallization. The mutated receptor evidenced enhanced thermostability and preferentially existed in an antagonist-binding state. Stretches of amino acid sequence were deleted from the N-terminal region (i.e., the loop connecting helices V and VI and the C-terminal region). A, the β_1-adrenergic receptor is colored by helix: helix I (blue), helix II (cyan), helix III (violet), helix IV (red), helix V (orange), helix VI (yellow), helix VII (green), and helix VIII (magenta). Thermostabilizing mutations (R68S, M90V, Y227A, A282L (not resolved in the shown structure), F327A, and F338M) and those that either increased functional expression (C116L) or eliminated a palmitoylation site (C358A) are shown as balls/sticks. B, structure of the β_1-adrenergic receptor (colored by helix) is shown with bovine rhodopsin (green ribbon) to illustrate key structural differences. Despite some differences in the transmembrane helices, the main distinction is in the organization of the cytoplasmic (C-) loops. The C-II loop in the β_1-adrenergic receptor structure forms a short α-helix, whereas this loop is more extended in rhodopsin. In addition, rhodopsin has a native C-III loop that is absent from the β_1-adrenergic receptor structure as a result of deletions needed for crystallization. C, the structure of the β_1-adrenergic receptor (colored by helix) is displayed with the human β2-adrenergic receptor (green ribbon) to show the key structural differences. In this case, the C-II loops of both the β_1- and β_2-adrenergic receptors are similar, but the α-helical conformation of the β_1-adrenergic receptor cannot be accommodated within the two crystallized structures of the β_2-adrenergic receptor because of lattice contacts with adjacent molecules. D, the structure of the β_1-adrenergic receptor (colored by helix) is displayed with the human A_{2A} adenosine receptor (green ribbon) to show key structural differences. The main difference between these two structures lies in the distinct folding of the extracellular loops, with the adenosine receptor adopting a more open surface for ligand binding as a result of this folding.

that forms a rigid, open structure, exposing the ligand binding cavity to solvent. The ZM241385 ligand in the crystallized adenosine receptor occupies a significantly different position than retinal and amine ligands, lying perpendicular to the membrane plane. This new structure indicates that the binding pocket in GPCRs can vary in position and orientation, permitting greater receptor diversity and ligand selectivity. We believe that this finding further highlights the need for high-resolution GPCR structural determinations, because the results of molecular modeling deviate significantly from the empiric data now available for the adenosine receptor.

GPCR Structure and Pharmacology

Although classic drug screening programs have been successful, more structural knowledge is needed for optimal drug design and improved therapy. The paucity of structural knowledge about GPCRs has severely limited the application of structure-based drug design (Lundstrom, 2006). Even though >30% of all marketed therapeutics act on GPCRs (Hopkins and Groom, 2002), these drugs target only ~30 members of this class, so there is enormous potential to exploit the remaining family members, including the >100 orphan receptors (Civelli, 2005), for which no existing ligands have yet been identified.

Even when a GPCR has high sequence homology and algorithms are used to predict its overall structure and possibly the location of the small-molecule binding site within the transmembrane domain with some accuracy, small differences in the exact helical arrangement may greatly affect the shape of the small-molecule binding site. For the many class A GPCRs that have a low sequence homology with bovine rhodopsin, the only native ligand bound GPCR structure known to date, homology models cannot accurately predict helical topography and, even less so, the topology of the small-molecule binding site (Schlyer and Horuk, 2006). This problem further highlights the need for native ligand-bound states of GPCRs to improve drug design. The structures of β_1- and β_2-adrenergic receptors, although informative on a global scale, lack this native binding property, and the new fusion A_{2A} adenosine receptor illustrates how empiric data can be in stark contrast to the predictive molecular modeling data concerning the actual ligand binding pocket. Improved expression and purification methods are badly needed to obtain high resolution structures in their native conformations for optimal drug design.

What Have We Learned about GPCRs from Their Structures?

Several additional points are worth mentioning:

1. It is remarkable how similar the overall structures of rhodopsin, adrenergic, and adenosine receptors really are. This fact is easily forgotten when relatively minor differences are featured in each new elucidated structure. For all rhodopsin structures, root-mean-square displacements for transmembrane regions are within 1.8 Å of each other, and even when the adrenergic receptors are compared with rhodopsin, these displacements are 3.3 to 3.5 Å for β_2-adrenergic receptor and 4.3 to 4.7 Å for β_1-adrenergic

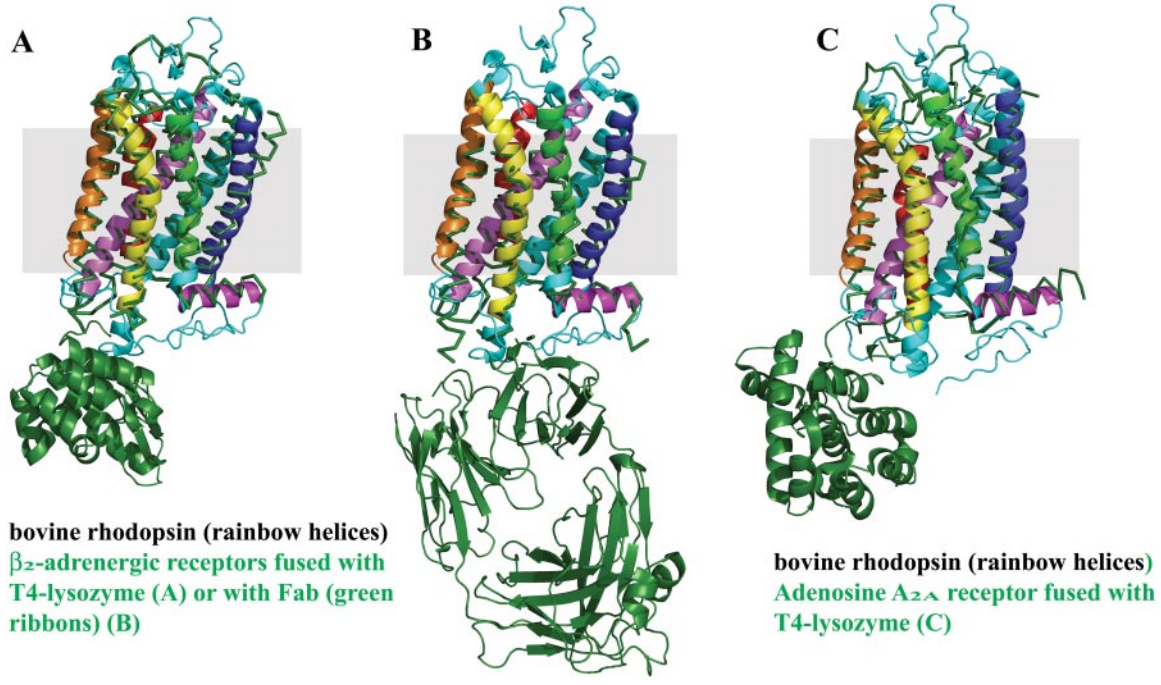

Fig. 6. Structural comparison of the β_2-adrenergic and A_{2A} adenosine fusion receptors with rhodopsin. Shown are structures of the human β_2-adrenergic receptor fused to T4 lysozyme (A) and in complex with Fab (B) and the human A_{2A} adenosine receptor fused to T4 lysozyme (C). Bovine rhodopsin is colored by helix: helix I (blue), helix II (cyan), helix III (violet), helix IV (red), helix V (orange), helix VI (yellow), helix VII (green), and helix 8 (magenta), whereas each of the two fusion β_2-adrenergic receptors are displayed as green ribbons. There are differences in the transmembrane helices between the β_2-adrenergic receptor and rhodopsin, with the most pronounced disparity occurring in helix I because the Pro residue kink is absent in the β_2-adrenergic receptor structures. In addition, the β_2-adrenergic receptor structures show minimal inter-receptor contacts illustrating that protein engineering may have affected the crystal packing and disrupted any possible dimeric interfaces of these structures. The overall helical differences between the adenosine receptor and rhodopsin are minimal, but the adenosine receptor has a distinct arrangement of the extracellular loops for a more open structure of the ligand binding pocket that is shifted closer to helices VI and VII.

receptor—closer to rhodopsin than to each other (D. Lodowski, unpublished observations). This close superimposeability occurs, in large part, because of the similar structures of interacting proteins such as the G proteins, receptor kinases, and arrestins. Despite differences in overall sequence homology among GPCRs, this natural phenomenon allows the vast majority of these receptors to present a similar topography. Preservation of only a few essential features is likely to be required for the activation process and engagement with G proteins (Mirzadegan et al., 2003).

2. A large number of compounds can bind to each of the GPCRs, yet only a portion of this ligand binding results in receptor activation and coupling with partner proteins. Moreover, among these agonist-stimulated activations, full or partial activity can be achieved. These facts indicate that changes on the cytoplasmic surface lead to differing efficacy of these ligands in activating a particular GPCR. Overall, small changes within 2 to 6 Å observed for rhodopsins and anticipated for other receptors suggest that such subtle changes either directly lead to different receptor conformations or indirectly affect the extent of protonation/deprotonation of key residues (like these in the DRY motif region) on the cytoplasmic surface that are responsible for the efficacy of G protein coupling. For photoactivated rhodopsin, *meta*-stable photointermediates of the activated receptor can be differentiated in part from one another based on their protonation state. The spectrally and functionally distinct MII intermediate capable of activating the heterotrimeric G protein differs from its precursor photointermediates by taking up a proton from the bulk solvent that confers increased conformational flexibility (Salom et al., 2006b).
3. The inherent flexibility of GPCRs permits conformational changes to be triggered by ligand binding. Energy for such a transformation due to ligand binding is typically between 8 and 12 kcal/mol. Obviously, only a small fraction of this energy is required for activation, and thus large "rigid body movements" are very unlikely to occur because they are not supported by the energetics of this process. These examples show that even though embedding proteins in a lipid bilayer imposes several restrictions on their conformation and movement, membrane proteins still retain considerable flexibility and mobility that are intimately connected to their function. For class A GPCRs, movement of the kind imposed by the Pro residue in helix VI could be the only significant movement for part of this helix during activation. Stevens noted that the organization of helices in inactive forms of GPCRs are slightly different (Jaakola et al., 2008). It is tempting to speculate that these slight differences in helix organization are not sufficient for activation of these receptors. Thus, how does the allosteric activation of GPCRs take place?
4. Water molecules could be involved in the activation process by an already mentioned protonation/deprotonation mechanism. Many candidate water molecules have already been identified in GPCRs, so discussion of this critical point in GPCR signaling will be the focus of additional theoretical and experimental work. With the lack of major movements along the GPCR helices, water seems to be a logical choice to transmit the signal from the ligand binding site to the cytoplasmic surface through realigning the position of amino acid rotamers along pathways connecting these two sites.
5. Finally, membrane proteins often oligomerize because exposure of hydrophobic regions to water incurs a large energetic penalty. Moreover, immobilization and conformational constraints imposed on these proteins by their oligomerization would provide a stabilizing influence. Both oligomerization and dissociation to monomers can be described by two biophysical concepts that seem largely adequate to explain both the size and formation dynamics of these structures, as has been shown for syntaxin 1 oligomers (Periole et al., 2007). A detailed analysis of oligomerization and its energetics has recently been presented (Müller et al., 2008). Even transient self-association of membrane proteins will guarantee that sufficient time for catalysis or signaling is achieved. Studies of GPCR oligomerization have generated much passionate discussion (Chabre et al., 2003; Park et al., 2004; Salahpour and Masri, 2007). However, an overwhelming amount of data accumulated over the years support the concept that GPCRs function as oligomeric rather than monomeric receptors (Milligan, 2004; Park et al., 2004; Terrillon and Bouvier, 2004). This concept is slowly gaining recognition, even in structural studies of GPCRs that provide the intellectual basis for pharmacologically relevant allosteric regulators (Park et al., 2008b).

Conclusions

Progress in elucidating the structures of membrane-bound GPCRs has been astonishing despite considerable technical difficulties. X-ray diffraction of GPCR crystals provides a static snapshot of their structure that allows simultaneous imaging of the involved structural amino acids. It can be argued that GPCR crystals do not mimic native structures because they form in high concentrations of the precipitant resulting in internal crystal contacts that could deform the structure and prevent conformational alterations in response to changes in ligand occupancy. This concern is likely valid to some degree, even though the precipitants were selected because they are nondenaturing and crystals would never form from an assembly of differing protein conformations. Moreover, the examined structures are well hydrated (~70%) and the protein concentration within the crystals of rhodopsin is between 9 and 14 mM, not much above the 5 mM found in the native state (Nickell et al., 2007). Furthermore, detergent and residual or added lipids do provide a milieu sufficient in many cases to maintain the functional properties of GPCRs. Undoubtedly, however, there is a critical need to correlate X-ray crystallographic findings with the cellular properties of these receptors. Even though crystallography of membrane proteins is labor-intensive and time-consuming, there is no obvious substitute yet. For a receptor with dimensions of 75 × 45 × 30 Å and conformational changes within 1 to 6 Å, other methods with errors within these ranges or possible artifacts exceeding 10 Å derived from chemical modifications of examined proteins may not be too informative. There also is the concern that structural information gained from extensively engineered GPCRs may or may not be useful for rational drug design where the native human protein structure is critically needed.

Acknowledgments

We thank Dr. Leslie T. Webster Jr. (Case Western Reserve University) for valuable comments on the manuscript.

References

Becker OM, Shacham S, Marantz Y, and Noiman S (2003) Modeling the 3D structure of GPCRs: advances and application to drug discovery. *Curr Opin Drug Discov Devel* **6:**353–361.

Buczyłko J, Saari JC, Crouch RK, and Palczewski K (1996) Mechanisms of opsin activation. *J Biol Chem* **271:**20621–20630.

Chabre M, Cone R, and Saibil H (2003) Biophysics: is rhodopsin dimeric in native retinal rods? *Nature* **426:**30–31.

Cherezov V, Rosenbaum DM, Hanson MA, Rasmussen SG, Thian FS, Kobilka TS, Choi HJ, Kuhn P, Weis WI, Kobilka BK, et al. (2007) High-resolution crystal structure of an engineered human beta(2)-adrenergic G protein-coupled receptor. *Science* **318:**1258–1265.

Civelli O (2005) GPCR deorphanizations: the novel, the known and the unexpected transmitters. *Trends Pharmacol Sci* **26:**15–19.

Deupi X, Dölker N, López-Rodríguez ML, Campillo M, Ballesteros JA, and Pardo L (2007) Structural models of class A G protein-coupled receptors as a tool for drug design: insights on transmembrane bundle plasticity. *Curr Top Med Chem* **7:**991–998.

Drake MT, Shenoy SK, and Lefkowitz RJ (2006) Trafficking of G protein-coupled receptors. *Circ Res* **99:**570–582.

Drews J (2000) Drug discovery: a historical perspective. *Science* **287:**1960–1964.

Filipek S, Krzysko KA, Fotiadis D, Liang Y, Saperstein DA, Engel A, and Palczewski K (2004) A concept for G protein activation by G protein-coupled receptor dimers: the transducin/rhodopsin interface. *Photochem Photobiol Sci* **3:**628–638.

Filipek S, Stenkamp RE, Teller DC, and Palczewski K (2003a) G protein-coupled receptor rhodopsin: a prospectus. *Annu Rev Physiol* **65:**851–879.

Filipek S, Teller DC, Palczewski K, and Stenkamp R (2003b) The crystallographic model of rhodopsin and its use in studies of other G protein-coupled receptors. *Annu Rev Biophys Biomol Struct* **32:**375–397.

Fotiadis D, Liang Y, Filipek S, Saperstein DA, Engel A, and Palczewski K (2003) Atomic-force microscopy: rhodopsin dimers in native disc membranes. *Nature* **421:**127–128.

Gether U (2000) Uncovering molecular mechanisms involved in activation of G protein-coupled receptors. *Endocr Rev* **21:**90–113.

Hansen CL, Classen S, Berger JM, and Quake SR (2006) A microfluidic device for kinetic optimization of protein crystallization and in situ structure determination. *J Am Chem Soc* **128:**3142–3143.

Hansen CL, Skordalakes E, Berger JM, and Quake SR (2002) A robust and scalable microfluidic metering method that allows protein crystal growth by free interface diffusion. *Proc Natl Acad Sci U S A* **99:**16531–16536.

Hanson MA, Cherezov V, Griffith MT, Roth CB, Jaakola VP, Chien EY, Velasquez J, Kuhn P, and Stevens RC (2008) A specific cholesterol binding site is established by the 2.8 A structure of the human beta2-adrenergic receptor. *Structure* **16:**897–905.

Hopkins AL and Groom CR (2002) The druggable genome. *Nat Rev Drug Discov* **1:**727–730.

Hubbell WL, Altenbach C, Hubbell CM, and Khorana HG (2003) Rhodopsin structure, dynamics, and activation: a perspective from crystallography, site-directed spin labeling, sulfhydryl reactivity, and disulfide cross-linking, in *Advances in Protein Chemistry, Volume 63: Membrane Proteins* (Rees DC ed) pp 243–290, Academic Press Inc, San Diego.

Jaakola VP, Griffith MT, Hanson MA, Cherezov V, Chien EY, Lane JR, IJzerman AP, and Stevens RC (2008) The 2.6 angstrom crystal structure of a human a2a adenosine receptor bound to an antagonist. *Science*, in press.

Kawakami N, Miyoshi K, Horio S, and Fukui H (2004) Beta(2)-adrenergic receptor-mediated histamine H-1 receptor down-regulation: another possible advantage of beta(2) agonists in asthmatic therapy. *J Pharmacol Sci* **94:**449–458.

Klabunde T and Hessler G (2002) Drug design strategies for targeting G-protein-coupled receptors. *Chembiochem* **3:**928–944.

Kroeze WK, Sheffler DJ, and Roth BL (2003) G-protein-coupled receptors at a glance. *J Cell Sci* **116:**4867–4869.

Lander ES, Linton LM, Birren B, Nusbaum C, Zody MC, Baldwin J, Devon K, Dewar K, Doyle M, FitzHugh W, et al. (2001) Initial sequencing and analysis of the human genome. *Nature* **409:**860–921.

Li J, Edwards PC, Burghammer M, Villa C, and Schertler GFX (2004) Structure of bovine rhodopsin in a trigonal crystal form. *J Mol Biol* **343:**1409–1438.

Li L, Mustafi D, Fu Q, Tereshko V, Chen DL, Tice JD, and Ismagilov RF (2006) Nanoliter microfluidic hybrid method for simultaneous screening and optimization validated with crystallization of membrane proteins. *Proc Natl Acad Sci U S A* **103:**19243–19248.

Liang Y, Fotiadis D, Filipek S, Saperstein DA, Palczewski K, and Engel A (2003) Organization of the G protein-coupled receptors rhodopsin and opsin in native membranes. *J Biol Chem* **278:**21655–21662.

Liang Y, Fotiadis D, Maeda T, Maeda A, Modzelewska A, Filipek S, Saperstein DA, Engel A, and Palczewski K (2004) Rhodopsin signaling and organization in heterozygote rhodopsin knockout mice. *J Biol Chem* **279:**48189–48196.

Loll PJ (2003) Membrane protein structural biology: the high throughput challenge. *J Struct Biol* **142:**144–153.

Lu ZL, Saldanha JW, and Hulme EC (2002) Seven-transmembrane receptors: crystals clarify. *Trends Pharmacol Sci* **23:**140–146.

Lundstrom K (2006) Latest development in drug discovery on G protein-coupled receptors. *Curr Protein Pept Sci* **7:**465–470.

McKibbin C, Farmer NA, Jeans C, Reeves PJ, Khorana HG, Wallace BA, Edwards PC, Villa C, and Booth PJ (2007) Opsin stability and folding: modulation by phospholipid bicelles. *J Mol Biol* **374:**1319–1332.

Menon ST, Han M, and Sakmar TP (2001) Rhodopsin: structural basis of molecular physiology. *Physiol Rev* **81:**1659–1688.

Milligan G (2004) G protein-coupled receptor dimerization: function and ligand pharmacology. *Mol Pharmacol* **66:**1–7.

Mirzadegan T, Benkö G, Filipek S, and Palczewski K (2003) Sequence analyses of G-protein-coupled receptors: similarities to rhodopsin. *Biochemistry* **42:**2759–2767.

Müller DJ, Wu N, and Palczewski K (2008) Vertebrate membrane proteins: structure, function, and insights from biophysical approaches. *Pharmacol Rev* **60:**43–78.

Murakami M and Kouyama T (2008) Crystal structure of squid rhodopsin. *Nature* **453:**363–367.

Nakamichi H, Buss V, and Okada T (2007) Photoisomerization mechanism of rhodopsin and 9-cis-rhodopsin revealed by X-ray crystallography. *Biophys J* **92:**L106–L108.

Nakamichi H and Okada T (2006a) Crystallographic analysis of primary visual photochemistry. *Angew Chem Int Ed Engl* **45:**4270–4273.

Nakamichi H and Okada T (2006b) Local peptide movement in the photoreaction intermediate of rhodopsin. *Proc Natl Acad Sci U S A* **103:**12729–12734.

Nakamichi H and Okada T (2007) X-ray crystallographic analysis of 9-cis-rhodopsin, a model analogue visual pigment. *Photochem Photobiol* **83:**232–235.

Nickell S, Park PS, Baumeister W, and Palczewski K (2007) Three-dimensional architecture of murine rod outer segments determined by cryoelectron tomography. *J Cell Biol* **177:**917–925.

Okada T, Ernst OP, Palczewski K, and Hofmann KP (2001) Activation of rhodopsin: new insights from structural and biochemical studies. *Trends Biochem Sci* **26:**318–324.

Okada T, Le Trong I, Fox BA, Behnke CA, Stenkamp RE, and Palczewski K (2000) X-ray diffraction analysis of three-dimensional crystals of bovine rhodopsin obtained from mixed micelles. *J Struct Biol* **130:**73–80.

Okada T, Sugihara M, Bondar AN, Elstner M, Entel P, and Buss V (2004) The retinal conformation and its environment in rhodopsin in light of a new 2.2 angstrom crystal structure. *J Mol Biol* **342:**571–583.

Okada T, Takeda K, and Kouyama T (1998) Highly selective separation of rhodopsin from bovine rod outer segment membranes using combination of bivalent cation and alkyl(thio)glucoside. *Photochem Photobiol* **67:**495–499.

Palczewski K (2006) G protein-coupled receptor rhodopsin. *Annu Rev Biochem* **75:**743–767.

Palczewski K, Kumasaka T, Hori T, Behnke CA, Motoshima H, Fox BA, Le Trong I, Teller DC, Okada T, Stenkamp RE, et al. (2000) Crystal structure of rhodopsin: a G protein-coupled receptor. *Science* **289:**739–745.

Park JH, Scheerer P, Hofmann KP, Choe HW, and Ernst OP (2008a) Crystal structure of the ligand-free G-protein-coupled receptor opsin. *Nature* **454:**183–187.

Park PS, Filipek S, Wells JW, and Palczewski K (2004) Oligomerization of G protein-coupled receptors: past, present, and future. *Biochemistry* **43:**15643–15656.

Park PS, Lodowski DT, and Palczewski K (2008b) Activation of G protein-coupled receptors: beyond two-state models and tertiary conformational changes. *Annu Rev Pharmacol Toxicol* **48:**107–141.

Patny A, Desai PV, and Avery MA (2006) Homology modeling of G-protein-coupled receptors and implications in drug design. *Curr Med Chem* **13:**1667–1691.

Periole X, Huber T, Marrink SJ, and Sakmar TP (2007) G protein-coupled receptors self-assemble in dynamics simulations of model bilayers. *J Am Chem Soc* **129:**10126–10132.

Petrek M, Otyepka M, Banás P, Kosinová P, Koca J, and Damborský J (2006) CAVER: a new tool to explore routes from protein clefts, pockets and cavities. *BMC Bioinformatics* **7:**316.

Rasmussen SG, Choi HJ, Rosenbaum DM, Kobilka TS, Thian FS, Edwards PC, Burghammer M, Ratnala VR, Sanishvili R, Fischetti RF, et al. (2007) Crystal structure of the human beta(2) adrenergic G-protein-coupled receptor. *Nature* **450:**383–387.

Ridge KD and Palczewski K (2007) Visual rhodopsin sees the light: structure and mechanism of G protein signaling. *J Biol Chem* **282:**9297–9301.

Ruprecht JJ, Mielke T, Vogel R, Villa C, and Schertler GFX (2004) Electron crystallography reveals the structure of metarhodopsin I. *EMBO J* **23:**3609–3620.

Salahpour A and Masri B (2007) Comment on: Experimental challenge to a 'rigorous' BRET analysis of GPCR oligomerization. *Nat Methods* **4:**599–600; author reply 601.

Salom D, Le Trong I, Pohl E, Ballesteros JA, Stenkamp RE, Palczewski K, and Lodowski DT (2006a) Improvements in G protein-coupled receptor purification yield light stable rhodopsin crystals. *J Struct Biol* **156:**497–504.

Salom D, Lodowski DT, Stenkamp RE, Le Trong I, Golczak M, Jastrzebska B, Harris T, Ballesteros JA, and Palczewski K (2006b) Crystal structure of a photoactivated deprotonated intermediate of rhodopsin. *Proc Natl Acad Sci U S A* **103:**16123–16128.

Schadel SA, Heck M, Maretzki D, Filipek S, Teller DC, Palczewski K, and Hofmann KP (2003) Ligand channeling within a G-protein-coupled receptor—the entry and exit of retinals in native opsin. *J Biol Chem* **278:**24896–24903.

Scheerer P, Park JH, Hildebrand PW, Kim YJ, Krauss N, Choe HW, Hofmann KP, and Ernst OP (2008) Crystal structure of opsin in its G-protein-interacting conformation. *Nature* **455:**497–502.

Schertler GFX (2005) Structure of rhodopsin and the metarhodopsin I photointermediate. *Curr Opin Struct Biol* **15:**408–415.

Schlyer S and Horuk R (2006) I want a new drug: G-protein-coupled receptors in drug development. *Drug Discov Today* **11:**481–493.

Standfuss J, Xie G, Edwards PC, Burghammer M, Oprian DD, and Schertler GF (2007) Crystal structure of a thermally stable rhodopsin mutant. *J Mol Biol* **372:**1179–1188.

Stenkamp RE (2008) Alternative models for two crystal structures of bovine rhodopsin. *Acta Crystallogr D Biol Crystallogr* **64:**902–904.

Teller DC, Okada T, Behnke CA, Palczewski K, and Stenkamp RE (2001) Advances in determination of a high-resolution three-dimensional structure of rhodopsin, a model of G-protein-coupled receptors (GPCRs). *Biochemistry* **40:**7761–7772.

Terakita A, Yamashita T, Tachibanaki S, and Shichida Y (1998) Selective activation of G-protein subtypes by vertebrate and invertebrate rhodopsins. *FEBS Lett* **439:** 110–114.

Terrillon S and Bouvier M (2004) Roles of G-protein-coupled receptor dimerization. *EMBO Rep* **5:**30–34.

Travis GH, Golczak M, Moise AR, and Palczewski K (2007) Diseases caused by defects in the visual cycle: retinoids as potential therapeutic agents. *Annu Rev Pharmacol Toxicol* **47:**469–512.

Venter JC, Adams MD, Myers EW, Li PW, Mural RJ, Sutton GG, Smith HO, Yandell M, Evans CA, Holt RA, et al. (2001) The sequence of the human genome. *Science* **291:**1304–1351.

Warne T, Serrano-Vega MJ, Baker JG, Moukhametzianov R, Edwards PC, Henderson R, Leslie AG, Tate CG, and Schertler GF (2008) Structure of a beta1-adrenergic G-protein-coupled receptor. *Nature* **454:**486–491.

Wise A, Gearing K, and Rees S (2002) Target validation of G-protein coupled receptors. *Drug Discov Today* **7:**235–246.

Wong SK and Ross EM (1994) Chimeric muscarinic cholinergic - beta-adrenergic receptors that are functionally promiscuous among G-proteins. *J Biol Chem* **269:** 18968–18976.

Yu H, Kono M, McKee TD, and Oprian DD (1995) A general method for mapping tertiary contacts between amino acid residues in membrane-embedded proteins. *Biochemistry* **34:**14963–14969.

Address correspondence to: Dr. Krzysztof Palczewski, Department of Pharmacology, School of Medicine, Case Western Reserve University, 10900 Euclid Ave., Cleveland, Ohio 44106-4965. E-mail: kxp65@case.edu